# EXPERIMENTAL AND NUMERICAL ANALYSIS OF THE SINGLE DROPLET IMPACT ONTO STATIONARY ONES

N. Nikolopoulos[1,2], G. Strotos[2], K.S Nikas[2], A. Theodorakakos[3], M. Gavaises[4], M. Marengo[5], G.E. Cossali[5]

[1] Centre for Research and Technology Hellas, 4th km Ptolemais Mpodosakeiou, Ptolemaida, Greece
[2] Technological Education Institute of Piraeus, Mechanical Engineering Department, Fluid Mechanics Laboratory, 250 Thivon & P. Ralli str., Aegaleo, 12244, Greece
[3] Fluid Research Co. 49 Laskareos Str, 11472, Athens, Greece
[4] City University London, School of Engineering and Mathematical Sciences Northampton Square, EC1V 0HB, London, UK
[5] Dept. of Industrial Engineering, University of Bergamo, viale Marconi 5, 24044 Dalmine, Italy
[C]Corresponding author: Nikolopoulos Nikos, n.nikolopoulos@certh.gr, 4th km Ptolemais Mpodosakeiou, Ptolemaida, Greece

ABSTRACT

The present paper investigates experimentally and numerically the impact of a spherical water droplet onto a stationary sessile one lying onto a substrate. The experiments were performed with two different film thicknesses, three different We numbers and two surface contact angles (two substrates, aluminium and glass). For this purpose a CCD camera was used and the corresponding qualitative and quantitative characteristics regarding the time evolution of the phenomenon, such as the diameter and height of the evolving crown, were obtained by image analysis. The aforementioned investigation was extended applying also the V.O.F (Volume Of Fluid) numerical methodology for the prediction of the temporal evolution of the phenomenon, so as to identify important characteristics of the induced flow field, not easy to be measured. This permits the in depth understanding of the governing flow laws, which resemble to those in the case of a droplet impact onto shallow films. The governing Navier-Stokes equations are solved both for the gas and liquid phase coupled with an additional equation for the transport of the liquid interface. An unstructured numerical grid is used along with an adaptive local grid refinement technique, increasing the numerical accuracy along the liquid-gas interface with the minimum computational cost. The numerical model is validated against the corresponding experimental data showing a good agreement. The regimes of deposition and splashing are identified as a function of We number and of the maximum thickness of the steady film, which is affected by the surface wettability properties. Moreover, following an analysis of the controlling parameters describing the temporal evolution of the lamella spreading, the role of We and Oh numbers as also of the wetting contact angle were identified, providing analytical expressions for the main dimensions characterizing the phenomenon.

## INTRODUCTION

The sequential impact of droplets onto solid and/or liquid surfaces is an interesting phenomenon which can be found in many engineering applications such as metallurgical industry, surface cooling, fire suppression, electronic circuits, inkjet printing etc. The investigation of any related to droplet impacts phenomenon requires the examination of the most significant dimensionless numbers, such as the Weber number (We), the Reynolds number (Re) and the Froude number (Fr), defined as:

$$We = \frac{\rho_l U_0^2 D_0}{\sigma}, \quad Re = \frac{\rho_l U_0 D_0}{\mu_l}, \quad Fr = \frac{U_0^2}{g D_0} \tag{1}$$

Other dimensionless numbers often used, relevant to the aforementioned, are the Ohnesorge (Oh) and the Bond (Bo) number, defined as:

$$Oh = \frac{We^{1/2}}{\mathrm{Re}} = \frac{\mu_l}{\sqrt{\rho_l \sigma D_0}}, \quad Bo = \frac{We}{Fr} = \frac{\rho_l g D_0^2}{\sigma} \tag{2}$$

The present investigation examines the impact of a droplet onto a stationary one. The phenomenon is expected to be a combination of the phenomena observed during droplet impact either onto a solid wall and/or onto a shallow film. A brief review of the phenomena observed during droplet impact onto solid and liquid surfaces can be found in Rein 1993 [1], along with some representative numerical works related with these phenomena [2-7]. However, despite the in depth investigation of droplet impacts onto solid surfaces and films of various thickness, very few information can be found in the literature as far as droplet impact onto sessile ones is concerned. For this reason, this study is focused on the experimental and numerical investigation of a finite chain of water droplets (two and three droplets in a row, after reaching a stable shape) impinging on a solid wall under atmospheric conditions, where the impacting droplet velocity, the height of the pre-existing liquid film, and the wettability characteristics of the solid substrate are the controlling parameters. The main difference with the most common experiments of impact on uniform liquid films is related to the influence of wall wettability on this phenomenon. Such an influence is evidenced both on the thickness of the film formed by the previously impacted drops and on the dynamic contact angle, which influences the movement of the contact line after the impact of the last drop.

## EXPERIMENTAL SETUP

The experimental rig used for the experiments is shown in Fig. 1. It comprises of a drop generator made by a suspended needle positioned at a distance ranging between 150 and 440 mm from the solid wall and connected with a small water tank. The detachment of single droplets is achieved by a small pressure pulse produced by the opening of a solenoid valve. The droplet diameter was

measured after enlarging the falling droplet's pictures at various time instants. The mean value was equal to Do = 4.02 mm, with a repeatability better than 6%, while the impact velocities ranged between 1.7 and 2.8 m/s. Two different solid plates were used, of either aluminum or glass composition, in order to analyse the effect of wettability on the evolution of the phenomenon. In all cases, distilled water at approximately 20°C under atmospheric conditions was used. A charge-coupled device (CCD) camera (Colour PCO SensiCam, 1280 × 1024 pixels) and a short duration flash lamp (Strobe) were used in order to capture the evolution of the phenomenon at various time instants before and after impact. Calibration for size measurements was obtained from the image analysis of pictures of known dimension bodies (needles).

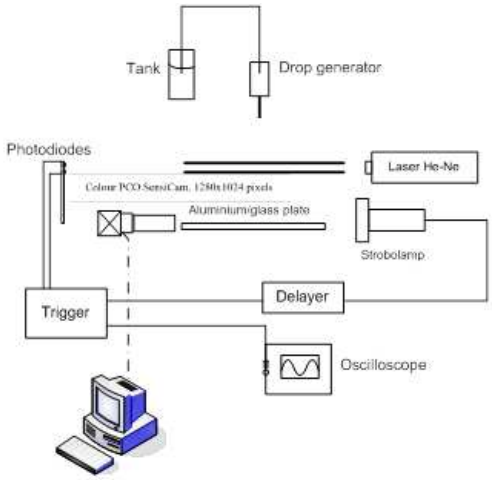


Figure 1: Drop impact test rig

| | Case | $D_0$ (mm) | $U_0$ | We | Re | Plate | δ=h/$D_0$ | ACA (°) |
|---|---|---|---|---|---|---|---|---|
| 2 droplets | A | 4.02 | 1.7 | 161 | 6800 | Aluminium | 0.215 | 60 |
| | B | 4.02 | 2.5 | 348 | 10000 | Aluminium | 0.23 | 60 |
| | C | 4.02 | 2.6 | 377 | 10400 | Aluminium | 0.234 | 60 |
| | D | 4.02 | 2.2 | 270 | 8800 | Glass | 0.130 | 10 |
| | E | 4.02 | 2.4 | 321 | 9600 | Glass | 0.146 | 10 |
| | F | 4.02 | 2.65 | 391 | 10600 | Glass | 0.120 | 10 |
| 3 droplets | A | 4.02 | 1.7 | 161 | 6800 | Aluminium | 0.329 | 60 |
| | B | 4.02 | 2.5 | 348 | 10000 | Aluminium | 0.277 | 60 |
| | C | 4.02 | 2.6 | 377 | 10400 | Aluminium | 0.266 | 60 |
| | D | 4.02 | 2.2 | 270 | 8800 | Glass | 0.140 | 10 |
| | E | 4.02 | 2.4 | 321 | 9600 | Glass | 0.180 | 10 |
| | F | 4.02 | 2.65 | 391 | 10600 | Glass | 0.162 | 10 |

Table 1: Examined cases, the number of droplets refer to those used to build the residual liquid bulk.

The image analysis of the experimental data allowed identification of at least two different regimes: (a) a deposition regime, with the formation of a crown but not followed by a breakup, and (b) a splashing regime characterized by the crown's breakup into numerous satellite droplets. Reasonably, an additional regime should exist for low impact velocities, where the impacting droplet deposits on the stationary liquid bulk, without the formation of any crown. This also occurs in the case of an impacting droplet onto a thin liquid film [8], but this regime was not investigated experimentally in the present paper.

Representative figures depicting the temporal evolution of droplet impact onto sessile ones are given in Fig.2a, 2b, 2c and 2d, but more information on these can be found in [9-10]. Table 1 reports the experimental conditions, in dimensionless form, for all the performed experiments. The time evolution of the phenomenon can be described by four main phases, whose characteristics can be distinguished from the relevant images. As shown in Fig. 2a, the droplets merge at once after their first contact, and the lamella's rim moves towards the liquid–solid contact line that, after being reached by the lamella, starts to move radially (compare the picture at 2.64 ms and 6.24 ms). During this spreading phase, the crown evolves radially and vertically. At subsequent times this crown evolves, as in the case of a droplet impacting onto a liquid film [11–13]. Dependent on the initial kinetic energy (impact velocity) and surface energy of the impacting droplet, this crown may either start collapsing without (deposition regime, Fig. 2a, t = 9.84–13.44 ms) or with (splashing regime, Fig. 2c, t = 2.75–9.52 ms) jetting phenomena and secondary droplets detachment.

During the final collapse, the surface energy is transformed back to kinetic energy under the effect of surface tension forces and gravity, and the crown begins to recede toward the solid substrate. For case A (low We, equal to 161) the formation of rim instabilities is observed, but no jets are produced because the kinetic energy is not high enough (Fig. 2a, t = 6.24 ms). Increasing the We number of the impacting droplets, the detachment of satellite droplets becomes more evident, even at the first stages of impact. This phenomenon shows similar characteristics to the "prompt" splash phase occurring in the case of a single droplet onto shallow films [11–13]. The remaining lamella later collapses for all cases examined, under the effect of gravity.

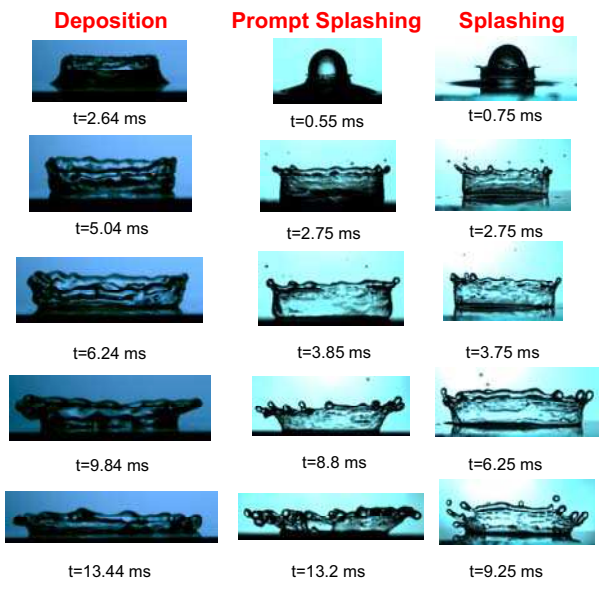

Figure 2: a) Temporal evolution of case A (2 droplets), b) Temporal evolution of case C (2 droplets), c) Temporal evolution of case F (2 droplets).

## NUMERICAL SETUP

Each phase (gas and liquid) is identified by the volume fraction α (ratio of liquid volume in a cell over the cell volume), following the Volume of Fluid Method (V.O.F) methodology by Hirt & Nichols [14]. The α-function is equal to 1 for a point of the computational domain inside the liquid phase, 0 inside the gas phase and lies between 0 and 1 in the gas-liquid interface. The discretization of the convection terms of the velocity components is based on a high resolution convection-diffusion differencing scheme (HR scheme) proposed by Jasak [15]. On the other hand, the discretization of equation of α needs a special treatment in order to avoid numerical diffusion and smearing of the interface. Thus, the high-resolution differencing scheme CICSAM proposed by Ubbink & Issa [16-17] is used and the time derivative is discretized using the second–order Crank-Nicolson scheme, as also small Courant number approximately 0.2-0.3. The non-linear system of the flow equations is solved numerically on a two-dimensional axisymmetric unstructured grid, using a recently developed adaptive local grid refinement technique, (Theodorakakos & Bergeles [18]), which enhances the accuracy at the interface region and achieves low computational cost compared to the case of a uniform grid with the same resolution.

A base grid is used and the cells at the region of the interface are subdivided according to the levels of local grid refinement used, while the interface lies always in the densest grid region since the grid is reconstructed every 10 timesteps. For the cases examined here, a base grid consisting of 3600 cells and 5 levels of local grid refinement was used. This resulted in a resolution of D0/516 at the interface region, which is found to be sufficient for a grid independent solution to be achieved after numerical tests. The number of computational cells varied from 17000 to 24000 (depending on the interface shape) while a uniform grid with the same resolution would require 3.68 million cells.

The time in the graphs presented will be non-dimensionalised as:

$$\tau = t \cdot \frac{U_0}{D_0} \qquad (3)$$

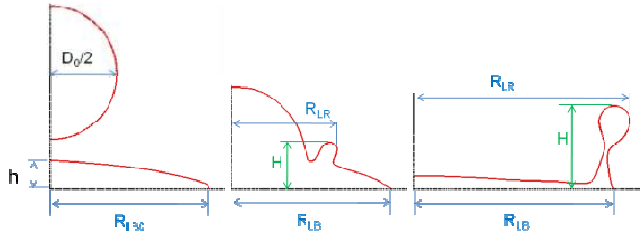


Figure 3a: Problem geometry and definition of the measured magnitudes.

Figure 3b: Longitudinal and azimuthal waves on the surface of the expanding crown, t=2.75ms and (b) satellite droplet detachment during the crown's collapse, t=6.75ms (case E, 3droplets).

### Crown's rim radius

The results obtained from the numerical simulation of the examined cases for the temporal evolution of crown's dimensionless radius are presented in Fig. 4a for the cases of 2 droplets and in Fig. 4b for the cases of 3 droplets. In these figures the left one (a) refers to the aluminum substrate and the right one (b) to the glass substrate. As it can be seen, the numerical predictions for the temporal evolution of crown diameter are in a good agreement with the corresponding experimental data and the deviations from the experimental data observed at later stages of the phenomenon, are attributed to the three-dimensional phenomena which become important and cannot be represented with validity by the present axisymmetric simulation. Fig. 4 reveals the invalidity of the axisymmetric numerical approach for the evolution of the phenomenon, after the time that three dimensional effects are evident.

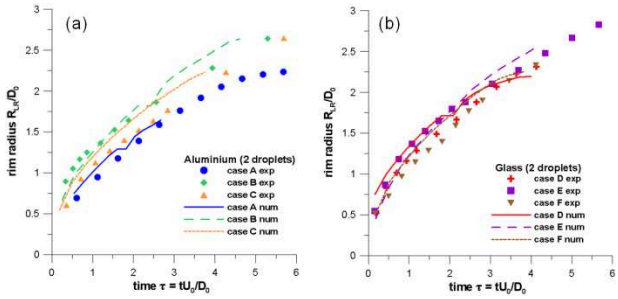


Figure 4a: Temporal evolution of rim's radius for impact on aluminium (a) and glass (b) substrate for the case of 2 droplets.

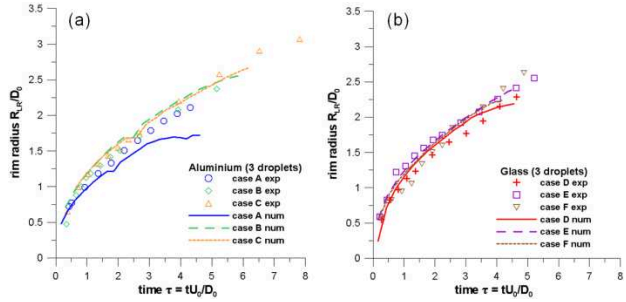


Figure 4b: Temporal evolution of rim's radius for impact on aluminium (a) and glass (b) substrate for the case of 3 droplets.

### Base radius

The results obtained from the numerical simulation of the examined cases as far as the temporal evolution of lamella's base dimensionless radius is concerned, are presented in Fig. 5a for the cases of 2 droplets and in Fig. 5b for the cases of 3 droplets. The results for the base radius are characterized by uncertainties in the experimental measurements. The predictions are in a good agreement with the corresponding experimental data, at the initial and middle stages of impact. At latter stages

discrepancies between experimental data and numerical results are owed to the three dimensional character of the phenomenon, which cannot be represented with validity by the present axisymmetric formulation of the physical problem. The base radius is almost constant until around to τ=2 and later the motion of the rim pushes the deposited lamella on the wall to move. That is the reason why there is a time delay for the base radius to increase. At later stages, which are not presented here, the deposited lamella on the wall recedes and finally reaches a stable form.

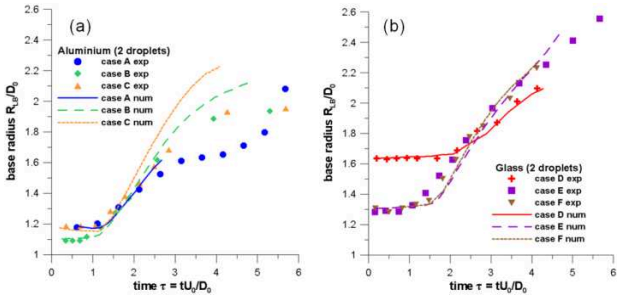


Figure 5a: Temporal evolution of base radius for impact on aluminium (a) and glass (b) substrate for the case of 2 droplets.

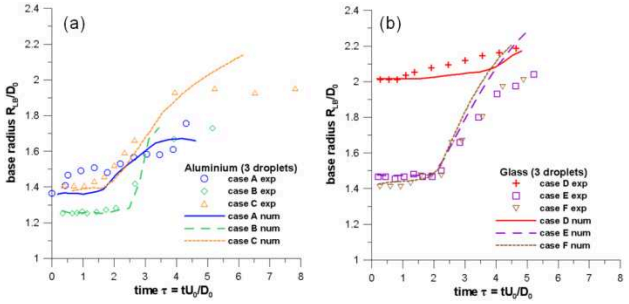


Figure 5b: Temporal evolution of base radius for impact on aluminium (a) and glass (b) substrate for the case of 3 droplets

## Crown's height

The results obtained from the numerical simulation of the examined cases for the temporal evolution of the non-dimensional crown's height are presented in Fig. 6a for the cases of 2 droplets and in Fig. 6b for the cases of 3 droplets. The height of the crown increases with time, reaches a maximum, and then decrease under the effect of gravity. The three dimensional character of the deposited lamella and the large fingers, which are inducing on its top rim cannot be represented by the present numerical approach owed to its axisymmetric form.

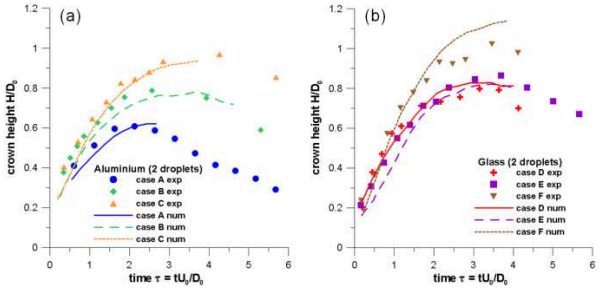


Figure 6a: Temporal evolution of crown's height for impact on aluminium (a) and glass (b) substrate for the case of 2 droplets.

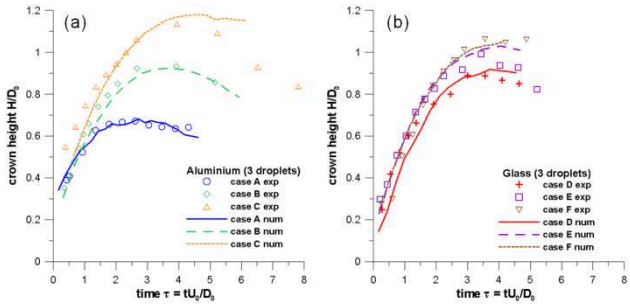


Figure 6b: Temporal evolution of crown's height for impact on aluminium (a) and glass (b) substrate for the case of 3 droplets.

## Flow field regimes

In this section, selected frames showing the temporal evolution of droplet shape, dimensionless pressure and dimensionless velocity are presented for cases A2 and F2 in Fig. 7, Fig. 8. Cases A and C have almost the same boundary conditions (2 droplets and aluminium surface) but different We numbers (We=161 and We=376 respectively), while cases C and F have similar We numbers but different boundary conditions regarding the shape of the sessile droplet. In these frames details of the flow field are also presented in enlarged pictures. The dimensionless pressure is presented in the left part of the pictures, while the dimensionless velocity magnitude is presented in the right part of the figures. These magnitudes are defined as:

$$p^* = \frac{p - p_\infty}{\frac{1}{2}\rho_l U_0^2}, \quad U^* = \frac{|\vec{u}|}{U_0} \tag{4}$$

For reasons of distinctness, a narrow range of values for pressure and velocity is presented despite the fact that at the initial stages of impact large values are observed for these magnitudes. Furthermore, the gas-liquid interface presented, corresponds to a VOF value equal to 0.5. For all cases, an advancing crown is created from the early stages of impact (Fig. 7. τ=0.613, Fig. 8. τ=0.317) originating from the peripheral points of the junction of the falling droplet with the sessile droplet. The crown moves radially outwards and vertically upwards and at its edge a thicker rim is formed (Fig. 7. τ=2.133, Fig. 8. τ=1.803). Its motion pulls the lower liquid mass to rise and the base of the sessile droplet increases.

At the initial stages of impact (τ≈0) the dimensionless pressure locally at the point of impact reaches a value of 6-7 and it is proved that the same value is observed for all cases, irrespective of impact velocity. This reveals the dimensionless character of the phenomenon as far as We number and wettability effects for the initial stages of the evolution of the phenomenon are concerned, at least for the range of parameters investigated in this paper. Later, within a short time interval of approximately τ=0.1-0.6 the maximum pressure is approximately equal to 1.8-2.5 (Fig. 8, τ=0.317) and its distribution in space is forming an oblique pressure gradient pointing from the axis of symmetry towards the rim of the crown (Fig. 7. τ=0.613-

1.120, Fig. 8. τ=0.704-1.803). This pressure gradient is responsible for the formation of the crown, since it pushes liquid mass in the diagonal direction, while the shear stress from the recirculating gas phase at this region, enhances the development of the crown. At subsequent times the pressure inside the liquid is further decreasing and exhibits a quite uniform distribution in space.

More information and details for the experiments and the numerical results can be found in [9,10].

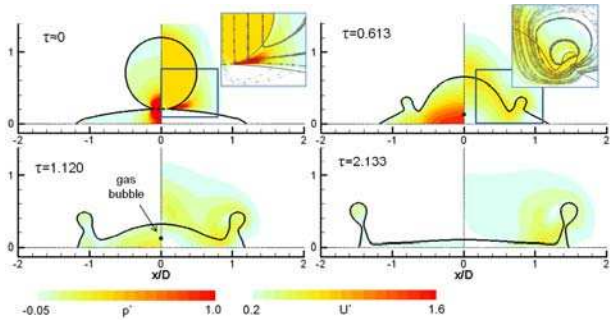


Figure 7: Selected frames of case A2 (We=161, Frh=340) showing the gas-liquid interface, the dimensionless pressure distribution (left hand side) and the dimensionless velocity distribution (right hand side). In the enlarged regions, representative streamlines are shown.

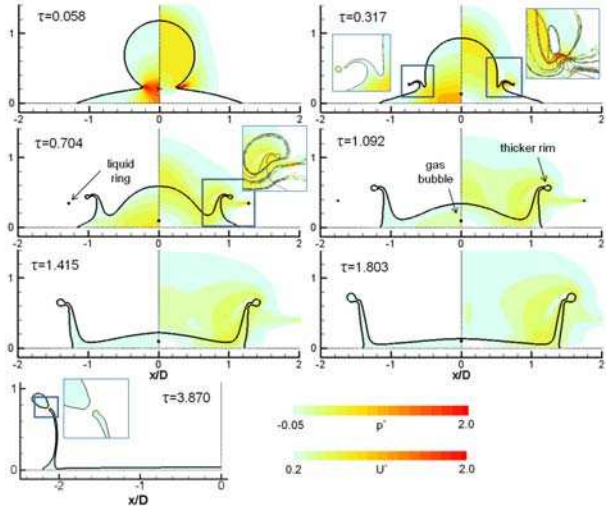


Figure 8: Selected frames of case F2 (We=391, Frh=1483) showing the gas-liquid interface, the dimensionless pressure distribution (left hand side) and the dimensionless velocity distribution (right hand side). In the enlarged regions, representative streamlines are shown.

## CONCLUSIONS

The experimental analysis of the measurements revealed that the governing physics of this type of phenomenon is quite similar to the one controlling the impact of a droplet onto shallow liquid films, although the influence of the wall wettability introduces some important differences in terms of the shape of the aforementioned liquid bulk. The crown rim diameter follows a law similar to the case of a droplet impingement onto a uniform film. The VOF methodology has been used to predict a set of experimental data presented in detail in the first part of this work. The phenomenon of droplet impact onto a sessile droplet was approached following an axisymmetric formulation of the governing equations, which is valid for the initial and intermediate stages of the evolution of the phenomenon, applying simultaneously an adaptive local refined unstructured grid. The predictions of the numerical model were in good agreement with the experimental data for the crown's dimensions and base diameter. Following the model validation a comprehensive discussion of the flow field regimes was presented. During the early stages of impact high pressure is built up at the points of impact and inside the liquid mass an oblique pressure gradient is developed, promoting the formation of the advancing crown. The initial pressure built-up is responsible for the entrapment of gas bubbles inside the liquid, whilst bubble rings were also identified. At later stages, three-dimensional phenomena, such as the disintegration of crown's rim into secondary droplets are predicted, thus allowing for the axisymmetric simulation of the phenomenon to be valid until three dimensional characteristics are evident.

## ACKNOWLEDGMENT

The financial grant of the European Commission through the Marie Curie Felloship (2003) and the support of UNIVERSITÀ DEGLI STUDI DI BERGAMO (Prof. M. Marengo, G.E. Cossali) are gratefully acknowledged.

## REFERENCES

[1] Rein M., *Phenomena of liquid drop impact on solid and liquid surfaces*, Fluid Dynamics Research, 12 (1993) 61-93.
[2] Nikolopoulos N., Theodorakakos A., Bergeles G., *Normal impingement of a droplet onto a wall film: a numerical investigation*, International Journal of Heat and Fluid Flow, 26 (2005) 119-132.
[3] Nikolopoulos N., Theodorakakos A., Bergeles G., *Three-dimensional numerical investigation of a droplet impinging normally onto a wall film*, Journal of Computational Physics, 225 (2007) 322-341.
[4] Nikolopoulos N., Nikas K.-S., Bergeles G., *A numerical investigation of central binary collision of droplets*, Computers & Fluids, 38 (2009) 1191-1202.
[5] Nikolopoulos N., Theodorakakos A., Bergeles G., *Off-centre binary collision of droplets: A numerical investigation*, International Journal of Heat and Mass Transfer, 52 (2009) 4160-4174.
[6] Strotos G., Nikolopoulos N., Nikas K.-S., *A parametric numerical study of the head-on collision behavior of droplets*, Atomization and Sprays, 20 (2010) 191-209.
[7] Nikolopoulos N., Theodorakakos A., Bergeles G., *A numerical investigation of the evaporation process of a liquid droplet impinging onto a hot substrate*, International Journal of Heat and Mass Transfer, 50 (2007) 303-319.
[8] Rioboo, R., Bauthier, C., Conti, J., Voue, M., and Coninck, J., *Experimental investigation of splash and*

*crown formation during single drop impact on wetted surfaces*, Exp. Fluids, 35:648–652, 2003.
[9] N. Nikolopoulos, G. Strotos, K.S. Nikas, A. Theodorakakos, M. Gavaises, M. Marengo, G. E. Cossali. *Experimental investigation of a single droplet impact onto a sessile drop*, Atomization and Sprays, 20(10), (2010), 909–922.
[10] N. Nikolopoulos. G. Strotos, K.S. Nikas, A. Theodorakakos, M. Gavaises, M. Marengo, G. E. Cossali. *Single droplet impacts onto deposited drops. Numerical analysis and comparison*, Atomization and Sprays, 20(10), (2010), 935–953.
[11] Cossali G.E., Coghe A., Marengo M., 1997, *The impact of a single drop on a wetted solid surface*. Experiments in Fluids, 22, 463-472
[12] Cossali G.E., Brunello G., Coghe A., Marengo M., 1999. *Impact of a single drop on a liquid film: experimental analysis and comparison with empirical models*. Italian Congress of Thermofluid Dynamics UIT, Ferrara 30 June.
[13] Cossali G.E., Marengo M., Coghe A., Zhdanov S., 2004. *The role of time in single drop splash on thin film*. Experiments in Fluids, 36, 888-900.
[14] Hirt C.W., Nichols B.D., *Volume of Fluid (Vof) Method for the Dynamics of Free Boundaries*, Journal of Computational Physics, 39 (1981) 201-225.
[15] Jasak H., *Error analysis and estimation for finite volume method with applications to fluid flows*, in, Ph.D Thesis, Imperial College of Science Technology & Medicine, University of London, 1996.
[16] Ubbink O., Issa R.I., *A method for capturing sharp fluid interfaces on arbitrary meshes*, Journal of Computational Physics, 153 (1999) 26-50.
[17] Ubbink O., *Numerical prediction of two fluid systems with sharp interfaces*, in, PhD Thesis, Department of Mechanical Engineering, Imperial College of Science, Technology & Medicine,University of London, 1997.
[18] Theodorakakos A., Bergeles G., *Simulation of sharp gas-liquid interface using VOF method and adaptive grid local refinement around the interface*, International Journal for Numerical Methods in Fluids, 45 (2004) 421-439.